Essential Readings in Light Metals: Aluminum Reduction Technology.
Edited by Geoff Bearne, Marc Dupuis and Gary Tarcy.

Light Metals

From *Light Metals 1985*, H.O. Bohner, Editor

BATH /FREEZE HEAT TRANSFER COEFFICIENTS:

EXPERIMENTAL DETERMINATION AND INDUSTRIAL APPLICATION

M.P. Taylor B.J. Welch

Department of Chemical and Materials Engineering
School of Engineering
University of Auckland
Auckland
NEW ZEALAND

Abstract

Electrolyte freezing stabilizes the operation of a smelting cell by protecting its sidewalls against erosion. However freezing can also occur during anode changing as the cold block is immersed and this is detrimental to the current distribution in the cell. In both processes a critical parameter is the convective heat flow to the freeze from the superheated electrolyte. Unfortunately this is difficult to determine from plant measurements because of dynamic variations in temperature and composition, while calculation of heat transfer coefficients from literature correlations has been hampered by inadequate knowledge of the thermal driving force and liquid flow pattern. In this paper experimental bath/freeze heat transfer coefficients are presented for both applications and, where possible, compared with theoretical predictions. Combining these coefficients with operating bath superheats enables the prediction of steady and transient ledging behaviour. The dynamic impact of freezing on anodes is also estimated from the transient measurements.

Introduction

Convective heat transfer between the molten and frozen phases of a smelting electrolyte is an integral feature of cell operation because of the low degree to which the bath is superheated above its liquidus point. Frozen ledge formation and stability on the sidewall (1) is often a determining factor in the cell's operating life (2) and the critical parameter in the analysis of ledging is the convective heat flow from the bath to the sidewall region (3,4). Despite fluctuations in metal height at the sidewall, the instantaneous heat transfer rate to a section of frozen ledge is controlled by the local heat transfer coefficient between the liquid and solid phases. The vertical ledge profile above the bath/metal interface must therefore reflect the variation in heat transfer coefficients down the wall as well as the increasing thickness and thermal resistance of carbon (monolithic sidewall construction). From the ledging and erosion profiles given in an earlier paper (1) it is evident that the convective and conductive resistances conspire to give a minimum ledge thickness (and maximum sidewall erosion) at a level marginally above the bath/metal interface. The local heat transfer coefficients at a vertical depth of 10-25 cm down the ledge surface are therefore of paramount importance and the main aim of the experimental investigation has been to provide free and forced convection data from which these plant projections can be made.

Another important objective of heat transfer studies is the determination of the dynamic effect of anode changing on the electrolytic process in the cell. It is known that some bath freezing does occur when the new, cool anode is immersed initially in the electrolyte. However the duration of this freezing and its effect on the anode current distribution in the cell has not been calculated and, to this end, a series of experiments has been performed to study the transient aspects associated with freezing and melting of bath on anodes. These experiments involved the rapid quenching of carbonaceous blocks in an electrolyte of typical smelter composition and allowed the extent and duration of bath freezing around the cooler solid objects to be determined. Because of the similarity between this process and anode immersion in the cell, the information obtained in the small scale tests can be applied directly to the anode changing operation and realistic estimates of the interruption in current flow to the new block are possible.

Experimental

The steady-state convection experiments required the maintenance of a permanent, thin layer of frozen cryolite on an internally cooled graphite cylinder which was situated in a crucible containing molten cryolite. Temperatures were measured inside the crucible, melt and graphite cylinder walls while the thickness of the frozen cryolite layer was determined by extracting the cylinder from the melt after a steady-state heat balance had been established. Further details of the procedure and heat transfer calculations are given elsewhere (5) since rotation of the cylinder (during forced convection measurements) required special instrumentation for the temperature readings.

The block quenching investigation involved immersing the specimen in the bath and observing the thermal response of the system, using rapid data acquistion (6), until steady-state was attained. The mass of frozen bath was determined at discrete intervals during immersion by withdrawing the specimen rapidly from the melt in a series of incremental quenching experiments. Comparison of the freezing trends for various sized blocks with the interchange of enthalpy between the furnace components showed that the bath

freezing, and therefore the bath/freeze heat flow, could be predicted during the transient process. A dimensionless correlation for the growth and decay of the frozen layer on the blocks also indicated that, for an electrolyte of known superheat, the extent and duration of the phase change process is a predictable function of the heat capacity and shape of the immersed object.

Convection to the Internally Cooled Graphite Cylinder

Within a cell, the velocities at the bath-ledge interface vary considerably (7,8). Thus it is necessary to determine heat transfer coefficients for the range of velocities expected and these have been computed from the steady-state laboratory study described elsewhere. When the cylinder was stationary a local Nusselt number - Rayleigh number relationship was established for the vertical freeze surface based on the following definitions:

$$Nu_x^1 = h_x^1 x / K_\ell \qquad (1)$$

$$Ra_x^1 = Pr \frac{g\beta (T_b - T_L) x^3}{\nu_\ell^2} \qquad (2)$$

where

h_x^1 = the local heat transfer coefficient between the bath and freeze at a depth, x, from the melt surface.

K_ℓ = the thermal conductivity of molten cryolite

Pr = the Prandtl number for cryolite

β = the volumetric coefficient of expansion

T_b = the melt temperature at a vertical depth, x.

T_L = the liquidus point of the melt (by cooling curve analysis)

ν_ℓ = the kinematic viscosity of molten cryolite

Equations (1) and (2) follow those given by Eckert (9) for convection in a rectangular enclosure of similar aspect ratio to that used here in the cylindrical geometry.

Regression on the local Nusselt numbers measured during free convective flow of bath down the freeze surface yielded the equation (corr coeff = 0.995):

$$Nu_x^1 = 0.39\ Ra_x^{1\ 0.29} \qquad (3)$$

in the Rayleigh number range : $10^4 < Ra_x^1 < 2 \times 10^7$. However interface velocities of the order of 10 cm/sec (as generated by rotation of the cylinder) caused the average heat transfer coefficient to increase from 608 $Wm^{-2}K^{-1}$ in natural convection to 880 $Wm^{-2}K^{-1}$ and also to become virtually independent of distance (x) from the melt surface. Forced convection therefore dominated the heat transfer under these conditions and the 45% increase in local heat transfer represents an upper limit for the impact of horizontal metal and bath velocities on the heat flow to the sidewall ledge.

The natural convection heat transfer in the bath adjacent to the sidewall has been estimated previously (10,11) using low temperature models in which the heat transfer corresponds to that measured on a vertical surface in a semi-infinite expanse of fluid. However the proximity of the anodes to the ledge and the ohmic heat generation which takes place beneath them indicates that the ledge is actually one side of a rectangular enclosure in which vertical recirculation of bath occurs as it is alternately heated at the anodes and cooled at the sidewall. Both the data of Eckert (9), and the experimental correlation obtained in this work (Eq.3), demonstrate that heat transfer by natural convection is considerably higher in low aspect ratio cavities (aspect ratio $\simeq 2$) than is predicted by the flat plate theory for an isolated vertical surface (12). Using the 'flat plate' Nusselt numbers, $(Nu_x)_{fp}$, as a benchmark for the fluid under consideration the enhancement in local heat transfer observed in the two studies can be compared:

$$\left.\begin{aligned} Nu_x^1\ (\text{Eckert}) &= 0.66\ Ra_x^{1\ 0.05}\ (Nu_x)_{fp} \\ Nu_x^1\ (\text{cryolite}) &= 0.83\ Ra_x^{1\ 0.04}\ (Nu_x)_{fp} \end{aligned}\right| \qquad (4)$$

At local Rayleigh numbers between 10^4 and 10^8, the increase is 5 - 66% for Eckert's data and 20 - 73% in the experiments with cryolite. Equation (4) defines the lower and upper bounds, respectively, for the natural convective heat transfer to the bath/ledge interface. Substitution of the flat plate relationship for the industrial bath (Prandtl No. of 14 compared to 9.9 for cryolite) into these limits yields the local Nusselt numbers over the critical 15 cm of ledge directly above the metal pad. Therefore, for a bath superheat of 10°C above the liquidus point, the average local heat transfer coefficients fall in the range:

$$450 < \bar{h}_x^1 < 480\ Wm^{-2}K^{-1} \qquad (5)$$

The free convection coefficients given in equation (5) are heavily influenced by the two externally forced flows which are superimposed on the vertical circulation pattern. A downward movement of bath at the sidewall is induced (13) by the anode gas evolution near the centre of the cell and this assists the natural convection current already present. Calculation of the heat transfer due to aiding, free and forced flows indicates that the combination will produce an enhancement over the existing free convection of approximately 20% (14) here. In addition to this the magnetic stirring of the metal pad can cause horizontal bath velocities higher than 0.1 ms^{-1} (7) adjacent to the ledge and under these conditions the 45% increase in local heat transfer observed during rotation of the experimental freeze layer (at a peripheral velocity of 0.12 ms^{-1}) should be applicable in practice. The assumption of a horizontal velocity equal in magnitude to the gas induced, vertical bath velocity (11) yields an increase of only 20% however and the two figures again represent the extremes between which the actual heat transfer coefficients will lie. Application of the corrections for forced convection to the natural convection coefficients in equation (5) gives:

$$650 < \bar{h}_x^1 < 830 \quad Wm^{-2}K^{-1}$$

Mathematical modelling of the heat flow to the frozen ledge has been performed (4) using measured bath and ledge interface (liquidus) temperatures (1). The resulting simulation of dynamic ledging behaviour on the sidewall

is shown in Figure 1 for bath/freeze heat transfer coefficients at either end of the calculated range given above.

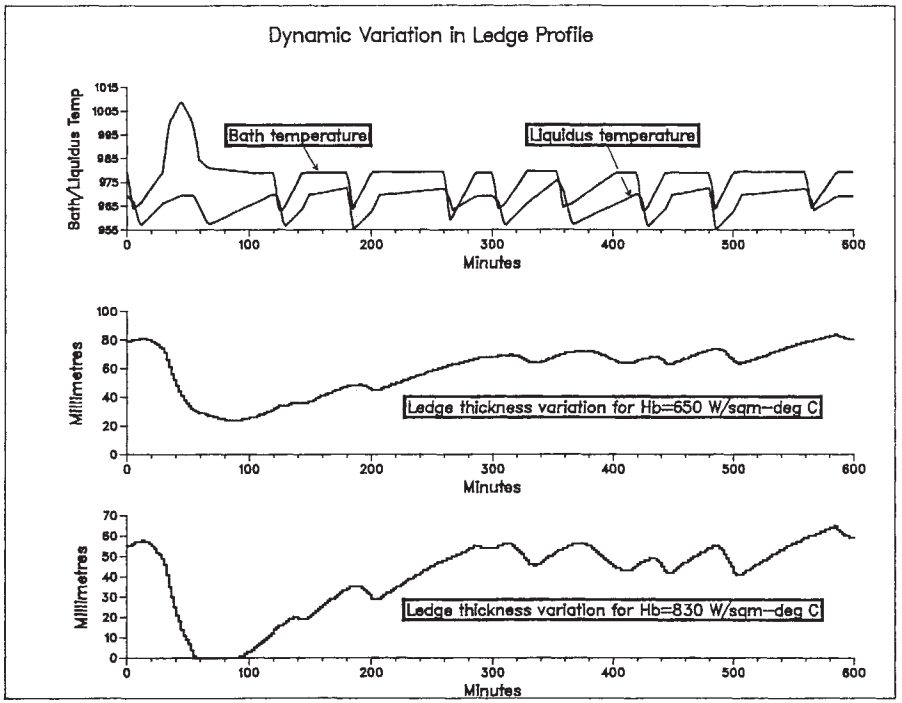

Figure 1 - Comparison of the Ledge Thickness Variation during a Ten Hour Simulation of Cell Operation for two values of the Bath/Ledge Heat Transfer Coefficient (Hb).

During the ten hour period of operation regular alumina feeding cycles, along with one manually terminated anode effect, are envisaged to occur and the shell temperature is maintained at 300°C by ambient air flow around the cell. The critical nature of the sidewall heat balance is evident from the two simulated ledge trends. A moderate heat transfer coefficient at the solid/liquid interface will allow the ledge to remain substantially intact during process disturbances and offer adequate protection to the sidewall against erosion. This contrasts markedly with the ledge protection offered in the higher heat transfer case in which the sidewall is exposed to molten metal and bath for approximately 35 minutes. Such a situation could easily arise at a corner block position on the upstream wall (for current flow) of end riser cells where the metal heave is often severe. The stability of the ledge at these locations is of greatest significance since sidewall tapout through erosion need only occur in one place for complete cell failure. It is therefore recommended that heat transfer coefficients near the upper end of the calculated range be applied in the analysis of sidewall ledging.

The Dynamic Impact of Anode Replacement

The growth and decay of the freeze layer in the small scale block quenching tests was generalized to an object of arbitrary shape and heat capacity for application to larger scale operations such as anode changing. Immersion time, t, was non-dimensionalized in the Fourier number:

$$Fo = \alpha t/R^2 \qquad (7)$$

where α is the thermal diffusivity of the quenched block and R is its volume to surface area ratio:

$$R = V/A \qquad (8)$$

The frozen mass present on the block at any time was expressed as the ratio of the latent heat supply, E_s, to the total energy demand, E_d, of the encapsulated object, multiplied by a shape factor, S:

$$S(E_s/E_d) = S \quad \frac{\rho_f V_f(t)\lambda_f}{(\rho VC + \rho_f V_f(t) C_f)(T_L - T_o)} \qquad (9)$$

where ρ_f, C_f and λ_f are the density, specific heat capacity and latent heat of the frozen electrolyte respectively. S is the surface area to volume ratio of the object referenced to that of a sphere with the same volume and is given by the equation:

$$S = \frac{1/R}{3/\left[\frac{3}{4\pi} V\right]^{\frac{1}{3}}} \qquad (10)$$

When the mass-time profiles were plotted as $S(E_s/E_d)$ versus Fourier number, the quenching experiments were reduced to a standard freezing-melting curve. Measured and computed mass-time profiles are compared in Figure 2(a) for two specimens and in Figure 2(b) the data is converted to the generalized coordinates using equations (7) and (9).

The maximum extent of the phase change process can be predicted from the dimensionless correlation in Figure 2(b):

$$S(E_s/E_d)_{max} = 0.25 \qquad (11)$$

Given a 400 Kg anode of cross-section 57x80cm, with an initial preheat (T_o) of 200°C, equation (11) indicates that immersion to a depth of 15 cm will cause 170 kg of bath to freeze around the bottom and sides of the anode. Final remelting of the freeze can be predicted by equating the total convective heat transfer with the enthalpy increase of the immersed anode since the phase change provides no net contribution to the heat balance:

$$Hb(T_o - T_L)At_{remelt} = \rho VC(T_L - T_o) \qquad (12)$$

Remelting times between one and five hours can be calculated from equation (12) depending on whether the whole anode or just the immersed section is assumed to contribute to the capcitive heat drain on the electrolyte. A lower superheat would be expected to cause even greater freezing around the block. In practice the amount of freezing is consideralby less as it is limited by the depth of melt under the anodes (4-5 cm) and the highly superheated metal pad lies immediately below.

(a)

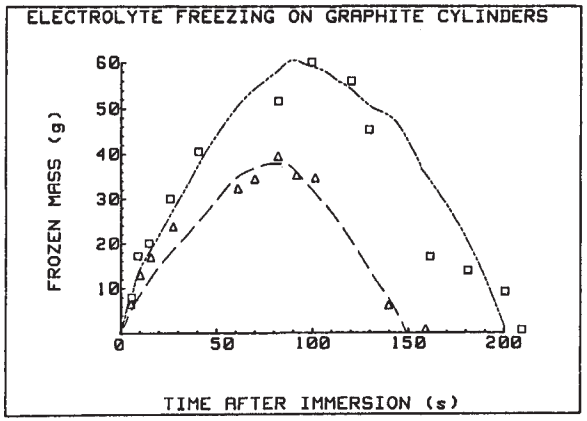

(b)

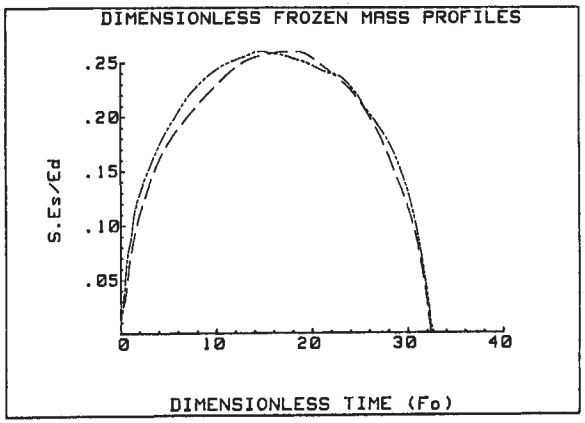

Figure 2(a) Comparison of the Experimentally Measured Freezing Trends with Computer Predictions for two specimens.

Computer Model: 25g cylinder — — —
41g cylinder —·—

Experiment: 25g cylinder △
41g cylinder □

Figure 2(b) The Computer Generated Freezing-Melting Trends after reduction to Dimensionless parameters using equations (7) and (9). Definition of the Model Curves is the same as for Figure 2(a).

Since the maximum freeze mass given above corresponds to 7 cm of solid bath around the anode, it is evident that all the electrolyte beneath a freshly immersed anode will solidify. Although the proximity of heat generation under neighbouring anodes would tend to reduce the lifetime of the freeze layer, this effect is more than offset by vertical conduction of heat into the upper two thirds of the anode which are not immersed in the bath. Obviously, setting an anode too high is seriously disadvantageous as it allows a greater thickness of freeze to grow before it strikes the metal pad. However any degree of bath freezing will cause current flow to be impeded by the electrically insulating solid layer on the underside of the anode. It is inevitable, therefore, that anode changing will be accompanied by an interruption in current flow to the new block lasting between one and five hours. At one anode replacement per day this represents a significant disruption to the overall current distribution in the cell and may be a contributing factor to the instability of the molten aluminium pad. The greater the metal pad curvature, the worse the effect will be.

References

1. Taylor,M.P., Welch, B.J., Keniry, J.T., "Influence of Changing Process Conditions on the Heat Transfer During the Early Life of an Operating Cell", AIME Light Metals, 437 (1983).

2. Peacey, J.G., Medlin, G.W., "Cell Sidewall Studies at Noranda Aluminium", AIME Light Metals, 1, 475 (1979).

3. Taylor, M.P., Welch, B.J., Keniry, J.T., "Effect of Electrochemical Changes on the Heat Balance in Aluminium Smelting Cells", J. Electro-analytical Chem., 168, 179 (1984).

4. Taylor, M.P., Welch, B.J., O'Sullivan, M.J., "Sidewall Ledge Dynamics in Cells Used for Electrowinning Aluminium", Chemeca 83 - Proc. 11th Aust. Chem. Eng. Conference, Brisbane, 493 (1983).

5. Taylor, M.P., Ph.D. Thesis, University of Auckland, Auckland, New Zealand (1984).

6. Taylor, M.P., Welch, B.J., McKibbin, R., "Effect of Convective Heat Transfer and Phase Change on the Stability of Aluminium Smelting Cells", paper presented at the AIChE Annual Meeting, San Francisco, 25 - 30 Nov. 1984.

7. Berge, B., Grjotheim, K., Krohn, C., Naeumann, R., Torklep, K., "Recent Studies of the Convection in Commercial Aluminium Reduction Cells", AIME Light Metals, 1, 57 (1973).

8. Robl, R.F., "Metal Flow Dependence on Ledging in Hall-Heroult Cells", AIME Light Metals, 449 (1983).

9. Eckert, E.R.G., Carlson, W.O., "Natural Convection in an Air Layer Enclosed Between Two Vertical Plates with Different Temperatures", Int. J. Heat and Mass Transfer, 2, 106 (1961).

10. Dernedde, E., Cambridge, E.L., "Gas Induced Circulation in an Aluminium Reduction Cell", AIME Light Metals, 1, 111 (1975).

11. Solheim, A., Thonstad, J., "Heat Transfer Coefficients Between Bath and Side Ledge in Aluminium Cells. Model Experiments", AIME Light Metals, 425 (1983).

12. Ostrach, S.,"An Analysis of Laminar Free-Convection Flow and Heat Transfer About a Flat Plate Parallel to the Direction of the Generating Body Force", National Advisory Committee for Aeronautics, Report 1111 (1953).

13. Haupin, W.E., "Calculating Thickness of Containing Walls Frozen from Melt", AIME Light Metals, 1, 188 (1971).

14. Lloyd, J.R., Sparrow, E.M., "Combined Forced and Free Convection Flow on Vertical Surfaces", Int. J. Heat and Mass Transfer, 13, 434 (1970).